http://dx.doi.org/10.5012/bkcs.2012.33.2.589

Quasi-classical Trajectory Calculation of the Chemical Reactions Ba+C_6H_5Br, *m*-$C_6H_4CH_3Br$

Wenwen Xia, Yonglu Liu,† Haiyang Zhong, and Li Yao*

Institute of Computational Physics, Department of Physics, Dalian Maritime University, Dalian 116026, P. R. China
**E-mail: yaoli@dlmu.edu.cn; haae@dlmu.edu.cn*
†Department of Military Ocean, Dalian Naval Academy, Dalian 116018, P. R. China
Received October 4, 2011, Accepted December 16, 2011

In this paper, the reactive dynamics properties of the reactions Ba + C_6H_5Br and Ba + *m*-$C_6H_4CH_3Br$ were studied by means of the quasi-classical trajectory method based on the London-Eyring-Polanyi-Sato potential energy surfaces. The vibrational distributions, reaction cross sections, rotational alignments of the products BaBr all were obtained. The peak values of the vibrational distributions are located at $v = 0$ for the reactions Ba + C_6H_5Br and Ba + *m*-$C_6H_4CH_3Br$ when the collision energies are 1.09 and 1.10 eV, respectively. The reaction cross sections increase with the increasing collision energy, which changes from 0.6 to 1.5 eV. The product rotational alignments deviate from −0.5 and firstly increase and then decrease while the collision energy is increasing, just like that of Heavy+Light-Light system.

Key Words : Reaction dynamics, QCT method, LEPS PES, Ba + C_6H_5Br reaction, Ba + *m*-$C_6H_4CH_3Br$ reaction

Introduction

With the rapid development of the experimental detection technology and the computational technology in recent decades, more and more people have focused their attentions on the dynamics researches and the discussions of the related reaction mechanisms for reactions between alkaline earth metal atoms and halide.[1-13] In the aspect of experiment, using the infrared chemiluminescence (CL), crossed molecular beam and laser-induced fluorescence (LIF) techniques can obtain detailed information of chemical reaction system, which provide an important experimental basis for revealing reaction process and studying reaction mechanism. Han *et al.* studied the reactions between atom Ba and halogenide in their experiments in Refs. (1)-(4).

At the same time, in the aspect of theory, a lot of studies on the reactions between alkaline earth metal atoms and halide were done, for example, those in Refs. (5)-(13). Currently, there are three theoretical methods mainly used to study the chemical reaction dynamics, which are the quasi-classical trajectory (QCT), the semi-classical, and the quantum theory methods. The QCT method is based on the molecular collision theory, which aims at simulating the movements of reactants on the potential energy surface (PES) by solving the classical Hamiltonian motion equations and this method has been used in order to reproduce the experimental results.

In 1990, Han *et al.*[1] studied the reactions Ba + $SiCl_4$/ + CH_3SiCl_3/ + $C_6H_5SiCl_3$ by means of the LIF method in a molecular beam equipment. They discussed the role of the released energies and the symmetries of the reagents by comparing with the reactions Ba + CCl_4/ + $CHCl_3$/ + CH_2Cl_2 in their paper. And in 1991, Han *et al.*[2] studied the reactions Ba + *o,m,p*-$C_6H_4Cl_2$ under the single collision condition using the LIF method and crossed molecular beam technology. They obtained the LIF spectra and relative reaction cross sections of the products BaCl. And vibrational distributions in Ref. (2) were obtained through the computational simulation. Han *et al.* considered that the rest of the energy turned into the vibration energy of the products BaCl after the bending vibration of the "export" transition state had turned into product rotation. In the same year, Lou *et al.*[3] produced the metastable atom Ba(^{3}D) by means of direct-current (DC) discharge method and studied the reactions Ba(^{3}D) + *o,m,p*-$C_6H_4Cl_2$/ + *o,m,p*-$C_6H_4CH_3Cl$, respectively. In their experiments, the electronically excited states of the products BaCl($A^2\Pi$, $B^2\Sigma$, $C^2\Pi$), the spectra, the total collision cross sections and the relative chemiluminescence reaction cross sections were obtained. They explained these experimental results by assuming that the reactions proceed *via* two channels in their paper. At the same time, Han and co-workers[4] studied the vibrational distributions and relative reaction cross sections of the products BaBr and BaI which were obtained from the reactions Ba + *p*-$C_6H_4INH_2$/ + *n*-C_4H_9I/ + C_6H_5Br/ + *m*-$C_6H_4BrCH_3$ and n-C_4H_9Br by means of the LIF method in a beam-gas arrangement. Through the experiments, they found that the vibrational excitations and cross sections of the reactions Ba + *m,p*-$C_6H_4CH_3Br$ were smaller than those of the reaction Ba + C_6H_5Br, but the vibrational excitations and cross sections of the reaction Ba + *p*-$C_6H_4INH_2$ were bigger than those of the reaction Ba + C_6H_5I.

In this paper, the QCT method was used to study the kinetic properties of the title reactions. The vibrational distributions, reaction cross sections and product rotational alignments were obtained through the calculations based on

the London-Eyring-Polanyi-Sato (LEPS) PESs. The theoretical calculation results in this work were compared with the experimental results[4] so as to give a reasonable explanation of the reaction mechanism on the theoretical level and predict the related results.

Theory

Potential Energy Surface (PES). In order to study the reaction mechanisms and dynamical properties of the title reactions, the first step is to construct the PES. Actually, the accurate *ab initio* PESs should be used to study the reaction mechanisms and dynamical properties of all of the reactions. However, since constructing an accurate *ab initio* PES is very difficult, the extended LEPS PES under the condition of the "quasi-three-atom" approximation was chosen to simulate the experimental results in this work. And the LEPS PES used here is on the ground state in the calculations.[14-17]

$$V(r_1, r_2, r_3)=Q_1 + Q_2 + Q_3-(J_1^2+J_2^2+J_3^2-J_1J_2-J_2J_3-J_1J_3)^{1/2} \quad (1)$$

where

$$Q_i = ({}^1E_i + {}^3E_i)/2 \quad (2)$$

$$J_i = ({}^1E_i-{}^3E_i)/2 \quad (3)$$

where ${}^1E_i$ is defined as the diatomic Morse potential function and ${}^3E_i$ stands for the anti-Morse function.

$${}^1E_i = D_i(\{1-\exp[-\beta_i(r-r_0)]\}^2-1) \quad (4)$$

$${}^3E_i = {}^3D_i(\{1+\exp[-\beta_i(r-r_0)]\}^2-1) \quad (5)$$

where

$${}^3D_i = D_i(1-S_i)/[2(1+S_i)] \quad (6)$$

where S_i is an adjustable parameter (so-called Sato parameter). D_i, β_i and R_i^0 are the Morse parameters of a diatomic molecule. In Han and co-workers' experiment paper,[4] the vibrational distributions were obtained through the computational simulations of the LIF spectra of the reactions Ba + C_6H_5Br and Ba + *m*-$C_6H_4CH_3Br$. In the QCT calculations, the Morse parameters mentioned above have to be used in the construction of the LEPS PES, but those parameters corresponding to the title reactions were not found in literatures. Therefore, in order to obtain the QCT results of the two reactions, the Morse parameters should be firstly obtained by means of the *Gaussian 03* program. In this paper, the *Gaussian 03* program on the B3LYP/lanl2dz level was used to optimize molecular structures and calculate frequencies. In the reaction processes, C_6H_5 and *m*-$C_6H_4CH_3$ can be seen as two groups of atoms whose internal configurations hardly change during the reactions, and the influences of their internal state excitation on the energy partition of the products can be neglected according to the calculations of the *Gaussian 03* program.[18] In this way, the reactions Ba + C_6H_5Br/ + *m*-$C_6H_4CH_3Br$ can be treated as the three-center collision reaction problems. Assuming that geometric constructions of C_6H_5 and *m*-$C_6H_4CH_3$ in the calculations are fixed, we mainly consider the inter-nuclear distances of Ba-Br, Ba-C and Br-C in optimizing the configurations. Energies of reactants, equilibrium bond lengths and force constants, all of which are used to construct the LEPS PESs in the QCT calculations, can be obtained from the following formulas.

$$D_i(AB) = (E_{HF}(A) + E_{HF}(B) - E_{HF}(AB)) \times 27.2116 \quad (7)$$

$$K_e = Frc \times 6.192 \quad (8)$$

$$\beta_i = \sqrt{\frac{K_e}{2D_i}} \quad (9)$$

Here, the dissociation energy D_i is in eV and the single point energy E_{HF} is in hartrees. In formula (7), *A* stands for atom Ba and *B* stands for atom Br. *Frc* is the force constant of the corresponding vibrational mode in mdyn/Å and K_e is the vibrational force constant in eV/Å^2.

Other important parameters in constructing the LEPS PESs are the adjusting Sato parameters S_i(i = 1, 2, 3) whose values change from −1.0 to 1.0. Subscript i = 1, 2, 3 respectively indicates Ba-Br, C_6H_5-Br (*m*-$C_6H_4CH_3$-Br) and C_6H_5-Ba (*m*-$C_6H_4CH_3$-Ba). Firstly, S_i(i = 1, 2, 3) are adjusted to simulate the experimental vibrational distributions. If the Sato parameters adjusted are suitable for the vibrational distribution result, the same Sato parameters will be used to calculate all the other results. The values of D_i, β_i, R_i^0 and the Sato parameters of the LEPS PESs constructed for the reactions Ba + C_6H_5Br and Ba + *m*-$C_6H_4CH_3Br$ are respectively presented in Tables 1 and 2.

In the calculations, a parameter named impact parameter *b*, which is used to indicate the degree of molecules approaching each other, needs to be considered. In order to study the collisions of all of the reaction atoms, the value of the maximum impact parameter b_{max} has to be determined and the result obtained under the condition of $b \le b_{max}$ can ensure

Table 1. The parameters used to construct the LEPS PES for the reaction Ba + C_6H_5Br

Species	D_i (eV)	β_i (Å^{-1})	R_i^0 (Å)	S_i
BaBr	2.7148	1.1698	3.2148	0.650
C_6H_5Br	3.1055	0.7755	1.9730	0.850
C_6H_5Ba	1.2044	0.6245	2.8508	0.350

The values of D_i, β_i, and R_i^0 were obtained by the *Gaussian 03* program at the B3LYP/lanl2dz level.

Table 2. The parameters used to construct the LEPS PES for the reaction Ba + *m*-$C_6H_4CH_3Br$

Species	D_i (eV)	β_i (Å^{-1})	R_i^0 (Å)	S_i
BaBr	2.7148	1.1698	3.2148	-0.100
m-$C_6H_4CH_3Br$	3.1064	0.7182	1.9755	0.150
m-$C_6H_4CH_3Ba$	1.1885	0.6078	2.8545	0.300

The values of D_i, β_i, and R_i^0 were obtained by the *Gaussian 03* program at the B3LYP/lanl2dz level.

Table 3. The calculated values of b_{max} for the reaction Ba + C_6H_5Br

E_{col}	0.6 eV	0.7 eV	0.8 eV	0.9 eV	1.0 eV	1.09 eV	1.2 eV	1.3 eV	1.4 eV	1.5 eV
b_{max}	5.05	5.40	5.80	5.80	5.85	5.90	5.85	5.80	5.75	5.80

The values of b_{max} for the reaction Ba + C_6H_5Br were calculated when the collision energy changed.

Table 4. The calculated values of b_{max} for the reaction Ba + *m*-$C_6H_4CH_3Br$

E_{col}	0.6 eV	0.7 eV	0.8 eV	0.9 eV	1.0 eV	1.1 eV	1.2 eV	1.3 eV	1.4 eV	1.5 eV
b_{max}	1.45	2.34	2.80	3.10	3.40	3.55	3.65	3.75	3.85	3.90

The values of b_{max} for the reaction Ba + *m*-$C_6H_4CH_3Br$ were calculated when the collision energy changed.

its accuracy. In this paper, b_{max} changes little with collision energies and the values are listed in Tables 3 and 4.

Quasi-classical Trajectory Calculation (QCT). The QCT method is most widely used in the molecular reaction dynamics studies. In this method, atomic nucleus in the reaction is considered as a classical particle and its motion can be described by the classical mechanics equation. Through the motion equation and statistical dispose, the micro and macro dynamics results of the reaction can be obtained. It is difficult to obtain the results of the Schrödinger equation for multi-atom system and the previous studies prove that the QCT calculation is good enough for the resolution of reaction dynamics problems, so the QCT method has been chosen in this work. The QCT method used here is the same standard as what it described in detail in Refs. (19)-(21). In order to reflect the macro-statistics of experiment and ensure the accuracy of calculation, the numerical integration was checked by the conservation of the total energy and total angular momentum. Then the Monte Carlo method was used to randomly select the representative trajectories in order to achieve the calculations of statistical distribution. The results of statistical distribution for the movement trajectories were used to obtain the theoretical result which can be compared with the experimental value. In the process of calculation, molecular internal energy states located at the initial and the end of the trajectory were treated as quantum states.

For the goal of calculation was to simulate the experimental results of the product state distribution, the same initial conditions with those of the experiment were selected. In the computations, collision energies were chosen as the average experimental values (1.09 and 1.10 eV). The initial inter-nuclear separations of atom Ba with the centre of mass of molecule C_6H_5Br or *m*-$C_6H_4CH_3Br$ were both chosen to be 15 Å in order to ensure that the interactions in Ba-C_6H_5Br and Ba-*m*-$C_6H_4CH_3Br$ can be neglected, and molecules R-Br (R=C_6H_5 or *m*-$C_6H_4CH_3$) were put on the levels of $v = 0$ and $j = 0$. 100,000 trajectories were sampled in the QCT calculations for each of collision energies and the integration step size was chosen to be 0.1 fs which can make the conservation of total energy and angular momentum.

Product Rotational Alignment. In the past 30 years, people have recognized that taking the properties of scalar and vector together into consideration in the study, they could obtain the complete kinetic information about reaction process. The vector correlation in the process of reaction $A + BC \rightarrow AB + C$, in particular, coupling between the reactant relative velocity vector and the product angular momentum is one of the most important vector correlations and it has been widely studied. The product rotational alignment was calculated in this paper by means of the computing code developed by Han *et al.*.[15]

For a general chemical reaction, the distribution of product rotational angular momentum $\vec{J}'$ relative to the reactant relative velocity vector $\vec{K}$ has the property of axial symmetry. This distribution is named rotational alignment and it can be described by the average value of the second item of the Legendre polynomial.

The total angular momentum is conserved during a reactive encounter,

$$\vec{J} + \vec{L} = \vec{J}' + \vec{L}' \tag{10}$$

where $\vec{L}$ and $\vec{J}$ are the orbital and rotational angular momenta of reagent, respectively. $\vec{L}'$ is the product orbital angular momentum. $\vec{L}$ plays an important role in producing the molecular distribution. According to the Impulse Model, Han and co-workers derived[22]

$$\vec{J}' = \vec{L}\sin^2\beta + \vec{J}\cos^2\beta + \vec{J}_Z(M_B/M_{AB}) \tag{11}$$

$$\vec{J}_z = 2(\mu_{BC}R)^{1/2}\vec{r}_{AB}\times\vec{r}_{CB} \tag{12}$$

where $\vec{J}_z$ is a contribution to $\vec{J}'$ which is caused by repulsive energy, μ_{BC} is the reduced mass of reagents *B* and *C*, $\vec{r}_{AB}$ and $\vec{r}_{CB}$ are vectors in the momentary reaction which are pointing from *B* to *A* and *C*, respectively, and $M_{AB}(=M_A + M_B)$ is the mass summation of reagents *A* and *B*. The reagents *A*, *B* and *C* mentioned in this paper represent atom Ba, atom Br and group C_6H_5 or *m*-$C_6H_4CH_3$, respectively. Approximately, the conditions $|\vec{L}| >> |\vec{J}|$ and $\cos^2\beta << \sin^2\beta$ can be generally satisfied by the mass factor, so the second term of Eq. (11) can be omitted. In other words, when $\vec{J}$ is small (as is common), $\vec{J}'$ can only result from $\vec{L}$. $\vec{J}'$ can be described by a function $f(\theta)$, in which θ denotes the angle between $\vec{J}'$ and *K*. $f(\theta)$ can be expanded in a set of Legendre polynomials:[23,24]

$$f(\theta) = \Sigma a_l P_l(\cos\theta) \tag{13}$$

And

$$a_l = \frac{2l+1}{2}\int_{-1}^{+1} P_l(\cos\theta) f(\cos\theta) d\theta \quad (14)$$

are the coefficient of the l-th Legendre polynomial. $l = 0$, 1, 2 respectively correspond to a_0, a_1 and a_2. a_0 is used to represent isotropy distribution. a_1 and a_2 are used to stand for rotational orientation and rotational alignment of product.

Customarily, $\langle P_2(\vec{J}'\cdot\vec{K})\rangle$ was used to represent the rotational alignment factor of product which was defined as:

$$\langle P_2(\vec{J}'\cdot\vec{K})\rangle = a_2/a_0 = 2.5\langle P_2(\cos\theta)\rangle/(0.5\langle P_0(\cos\theta)\rangle)$$
$$= \left\langle \frac{1}{2}(3\cos^2\theta - 1)\right\rangle \quad (15)$$

where P_2 is the second item of the Legendre polynomial and $\langle\cos^2\theta\rangle$ can be obtained by averaging over all of the directions and parameters of collision, and then the value of $\langle P_2(\vec{J}'\cdot\vec{K})\rangle$ can be obtained by means of the Eq. (15). Here the range of $\langle P_2(\vec{J}'\cdot\vec{K})\rangle$ is from −0.5 to 0.0. Therein the value equals −0.5 corresponding to the strongest rotational alignment of product. At this time, the direction of $\vec{J}'$ distributes within a small angle which is perpendicular to the direction of $\vec{K}$. In this paper, we only calculate the product rotational alignment, which has been measured in many experiments now.

Results and Discussions

Potential Energy Surface. Figure 1 and Figure 2 show the contour diagrams of the extended LEPS PESs for the reactions Ba + C_6H_5Br and Ba + *m*-$C_6H_4CH_3Br$, respectively. All of the following figures and results, given in this paper, were obtained from the QCT calculations based on those LEPS PESs according to the data in Tables 1 and 2. The reactions Ba + C_6H_5Br and Ba + *m*-$C_6H_4CH_3Br$ can be generally described as compound reactions. As can be seen from Figure 1 and Figure 2, the potential energies oscillate from the entrance ($R_{AB,C} = \infty$, corresponding to reactants) to the exit ($R_{AB,C} = \infty$, corresponding to products). Potential well is hardly involved in Figure 1 and Figure 2, but there are small reaction barriers for both of the reactions. The depth of the small reaction barrier for Ba + C_6H_5Br is 1.0 erg × 10^{16} (6.2415 × 10^{-5} eV) in Figure 1 and that for Ba + *m*-$C_6H_4CH_3Br$ is 9.034 erg × 10^{16} (5.6386 × 10^{-4} eV) in Figure 2. Both of them were obtained from the data of the LEPS PESs.

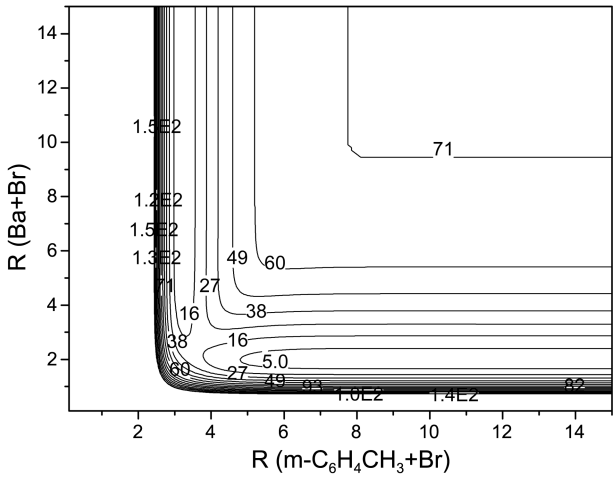

Figure 2. The plot of the LEPS PES for the reaction Ba + *m*-$C_6H_4CH_3Br$. The unit of R is Å and the unit of energy is in erg × 10^{16} (1 erg = 6.2415 × 10^{11} eV).

Vibrational Distribution. The comparisons between experimental and theoretical vibrational distributions of the products BaBr are shown in Figure 3 and Figure 4 for the reactions Ba + C_6H_5Br and Ba + *m*-$C_6H_4CH_3Br$, respectively. The vibrational distributions are expressed as a function of vibrational quantum number. The collision energies are chosen as 1.09 eV for the reaction Ba + C_6H_5Br and 1.10 eV for the reaction Ba + *m*-$C_6H_4CH_3Br$, which are the same as the experimental condition in Ref. (4). And the experimental results shown in Figure 3 and Figure 4 are directly derived from Figure 4 in Ref. (4). The vibrational distribution

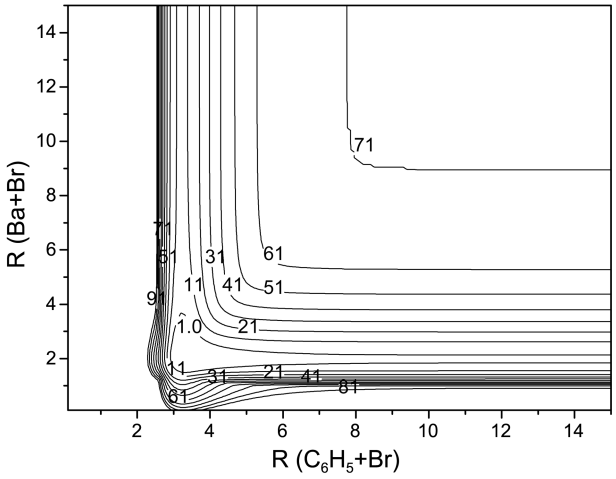

Figure 1. The plot of the LEPS PES for the reaction Ba + C_6H_5Br. The unit of R is Å and the unit of energy is erg × 10^{16} (1 erg = 6.2415 × 10^{11} eV).

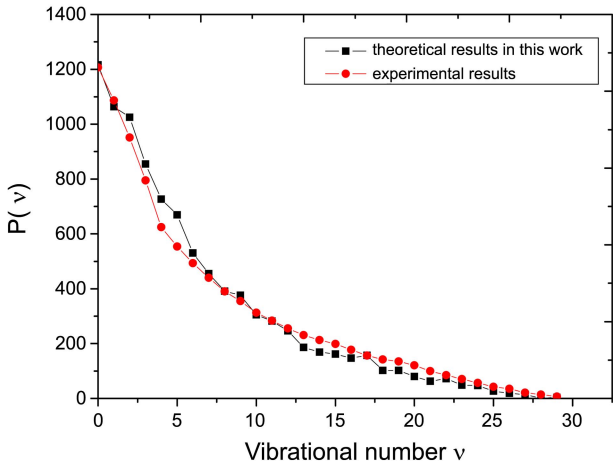

Figure 3. Vibrational distribution of product BaBr obtained from the reaction Ba + C_6H_5Br when collision energy equals 1.09 eV. The experimental result was obtained from Figure 4(a) in Ref. (4).

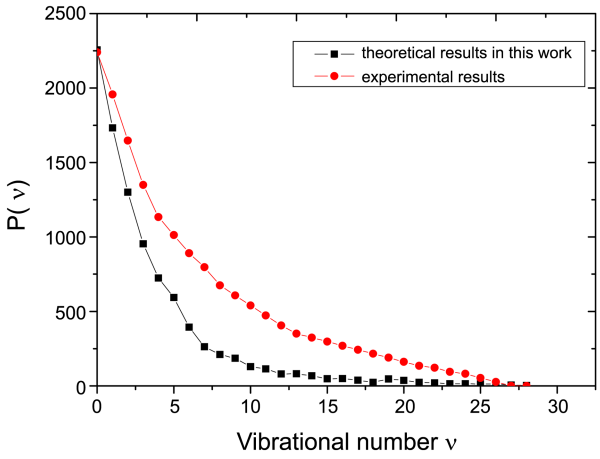

Figure 4. Vibrational distribution of product BaBr obtained from the reaction Ba + *m*-$C_6H_4CH_3Br$ when collision energy equals 1.10 eV. The experimental result was obtained from Figure 4(b) in Ref. (4).

results given in the experiment of Han and co-workers[4,25] were obtained through the computational simulations of the LIF spectra of the reactions Ba + C_6H_5Br and Ba + *m*-$C_6H_4CH_3Br$. The vibrational distribution results in this paper are obtained by the theoretical calculations by means of the QCT method which is based on the LEPS PESs.

In the two figures, the calculated vibrational distributions of the reactions show a gradual decrease in the whole range of vibrational quantum number. The peak values of the experimental distributions of the products BaBr appeared at around v = 0 for the two reactions in Refs. (4) and (25). And it can be seen from Figure 3 and Figure 4 that the maximum values of the vibrational distributions are also located at around v = 0 with the collision energies respectively at 1.09 and 1.10 eV in the theoretical results. Obviously, the calculated vibrational distributions of the products BaBr in the present work basically agree with the experimental results.[4,25]

The presence of methyl on benzene ring can weaken the activity of halogen atom.[4] The vibrational excitation of the product BaBr and the cross section obtained from the reaction Ba + *o,m,p*-$C_6H_4CH_3Br$ are smaller than those of the reaction Ba + C_6H_5Br.[4] For reactions of Ba with benzene halide or benzyl halide, the vibrational distributions of products BaX (X is halogen atom) are disperse, while for reactions of Ba with halogenated alkane, the vibrational distributions of products BaX are concentrated on their maximum values. These are due to the different mechanisms of the two types of reactions.

For the reaction between Ba and *m*-$C_6H_4CH_3Br$, the vibrational distribution of the product BaBr is almost independent of the relative position of atom Br with methyl. However, for the reactions between alkaline earth metal (M) atom and halogenated alkane, the vibrational distributions of products MX are determined not only by the position of X, but also by the relative positions of two or more halogen atoms in halogenated alkane.[4] If atom M approaches halogenated alkane from different directions, the vibrational distributions of products MX will also be different.[4] In other words, for the reactions of Ba with benzene halide or benzyl halide, the vibrational distributions of products hardly depend on the relative orientation of the reactants. But for the reactions between atom M and halogenated alkane, the vibrational distributions of products have strong dependence on the relative orientation.

As is known, the lowest unoccupied molecular orbit (LUMO) of benzene halide or benzyl halide is the π^* bonding orbit of benzene ring, and not the σ^* bonding orbit of carbon-halogen bond. This is different from halogenated alkane molecule. When atom M reacts with benzene halide or benzyl halide, electrons (*viz.* valence electrons of atom M) in the highest occupied molecular orbit (HOMO) firstly enter the π^* bonding orbit, then transfer to the σ^* bonding orbit of carbon-halogen bond through vibration coupling, and finally form the metal halide molecule. The previous experimental results[2] show that no matter from which direction that atom Ba collides with $C_6H_4Cl_2$, the probability of reaction is equal. It is believed that conjugated π bond on benzene ring can be regarded as "medium" during the reaction. So it is easy to explain that vibrational distribution of product has a weak dependence on the relative orientation among reactants.

Although the two calculated results of the products BaBr are in good agreement with the experimental results, some differences in the vibrational distributions can still be observed. These differences are probably due to the different conditions of this work and the experiment,[4] and the basic shortcomings of the models (the QCT method and LEPS PES) that have been chosen in this work. Actually, the small differences do not affect the analysis of reaction dynamics properties and reaction mechanism. And the dynamics results not given in the experiment[4] can be obtained through the QCT calculations in this paper. These theoretical results can provide more advantageous information for the research of reaction and forecast the experimental results.

Reaction Cross Section. The reaction cross sections of the products BaBr obtained from the reactions Ba + C_6H_5Br

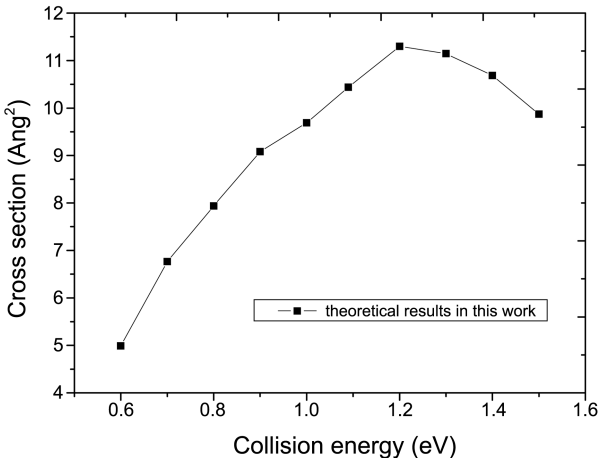

Figure 5. The reaction cross section result *versus* collision energy for the reaction Ba + C_6H_5Br.

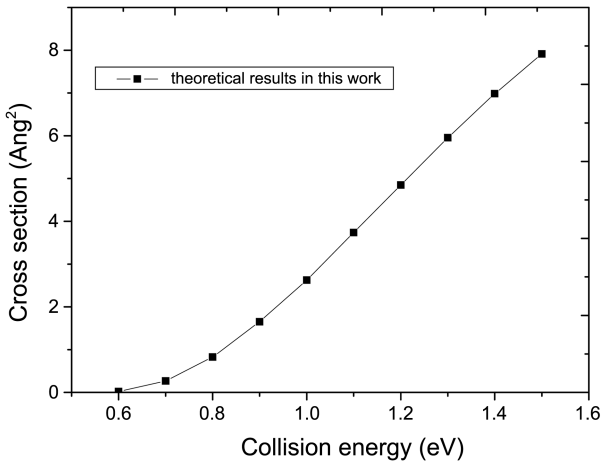

Figure 6. The reaction cross section result *versus* collision energy for the reaction Ba + *m*-$C_6H_4CH_3Br$.

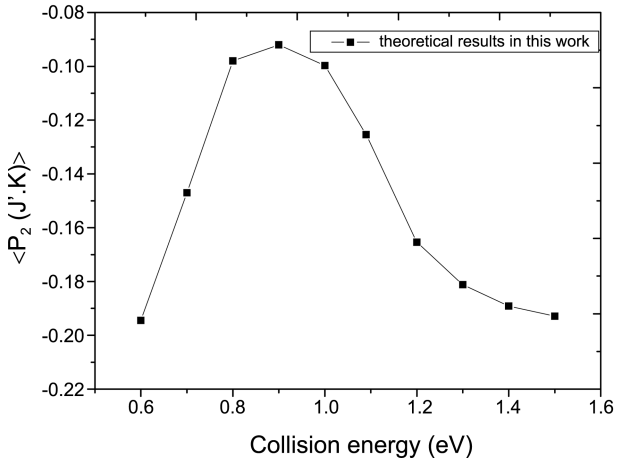

Figure 7. The product rotational alignment result of the reaction Ba + C_6H_5Br *versus* collision energy.

and Ba + *m*-$C_6H_4CH_3Br$ were calculated by means of the QCT method on the LEPS PESs and the formula can be written as follows,

$$\sigma_r = \pi b_{\max}^2 (N_r/N) \quad (16)$$

where N is the number of total trajectories calculated in this study and N_r is the number of reactive trajectory under the $b \le b_{\max}$ condition.

The results are obtained from Eq. (16) and given in Figure 5 for the reaction Ba + C_6H_5Br, and in Figure 6 for the reaction Ba + *m*-$C_6H_4CH_3Br$. As is shown in Figure 5, the reaction cross section regularly increases with the increasing of collision energy from 0.6 to 1.2 eV and reach its maximum value 11.30 Å^2 at collision energy of 1.2 eV. Then the values of the reaction cross section show a steady decrease *versus* the collision energy continuously increasing from 1.2 to 1.5 eV. In Figure 6, the range of the collision energy is also from 0.6 to 1.5 eV, but the result has a small difference from the reaction Ba + C_6H_5Br. As can be seen from Figure 6, the reaction cross section monotonously increases from the minimum to the maximum with the increasing of collision energy and reaches its maximum value when collision energy equals 1.5 eV. Meanwhile, from the comparison of the two results shown in Figure 5 and Figure 6, it can be found that the values of the reaction cross section for the reaction Ba + C_6H_5Br are larger than those of the reaction Ba + *m*-$C_6H_4CH_3Br$ with a methyl on the benzene ring.

Han and co-workers[4] concluded from the experiment that the ratio of the reaction cross sections between Ba + C_6H_5Br (σ_1) and Ba + *m*-$C_6H_4BrCH_3$ (σ_2) is σ_1/σ_2 = 3-5, and the presence of methyl on benzene ring decreases the activity of halogen atom. These phenomena can be qualitatively explained that the values of reaction cross section depend on the receptivity of electron on benzene ring, which mainly counts on the charged nature of benzene ring. Obviously, benzene ring with positive charge is easier to accept electron than electronegative benzene ring. Group CH_3 belongs to the electron-donating group and benzene ring tends to reveal electronegativity when methyl consists in it. For the reagent C_6H_5Br, benzene ring shows electropositivity, but when methyl substitutes for an atom H of C_6H_5Br, the positive charge of benzene ring will be neutralized to some extent and the receptivity of electron on benzene ring will become weak. So the values of reaction cross section for Ba + *m*-$C_6H_4CH_3Br$ are smaller than those for Ba + C_6H_5Br. Clearly, the relation of the reaction cross sections of the reactions Ba + C_6H_5Br and Ba + *m*-$C_6H_4CH_3Br$ is the same as that suggested in Refs. (3) and (4).

Product Rotational Alignment. In this study, not only the scalar properties but also the vector properties can be acquired from the QCT calculations. The rotational alignments of the products BaBr *versus* collision energy (0.6 to 1.5 eV) were calculated and the results are displayed in Figure 7 for the reaction Ba + C_6H_5Br and in Figure 8 for the reaction Ba + *m*-$C_6H_4CH_3Br$, respectively.

It can be seen from Figure 7 that the calculated values of $\langle P_2(\vec{J'} \cdot \vec{K}) \rangle$ for the reaction Ba + C_6H_5Br deviate from the kinematic limit value −0.5. The product rotational alignment rapidly increases to its maximum at E_{col} = 0.9 eV and then slowly decreases with the increasing of collision energy. The product rotational alignment values shown in Figure 7 are overall bigger than −0.5, and therefore the effects of product rotational alignment are not very strong for the reaction Ba + C_6H_5Br. It is very interesting to find that the variation tendency of the product rotational alignment for the reaction Ba + *m*-$C_6H_4CH_3Br$ is basically the same with that of the reaction Ba + C_6H_5Br. In Figure 8, the values of $\langle P_2(\vec{J'} \cdot \vec{K}) \rangle$ firstly increase with the increasing of collision energy until E_{col} = 1.0 eV and then decrease slightly under the condition of the continuous increase of collision energies. Different from the product rotational alignment of the reaction Ba + C_6H_5Br, the values in Figure 8 slightly deviate from −0.5, which means that the effects of the product rotational alignment for the reaction Ba + *m*-$C_6H_4CH_3Br$ are stronger than those for the reaction Ba + C_6H_5Br.

The reaction barrier leads to the results that the reaction cross sections increase with the increasing of collision energy

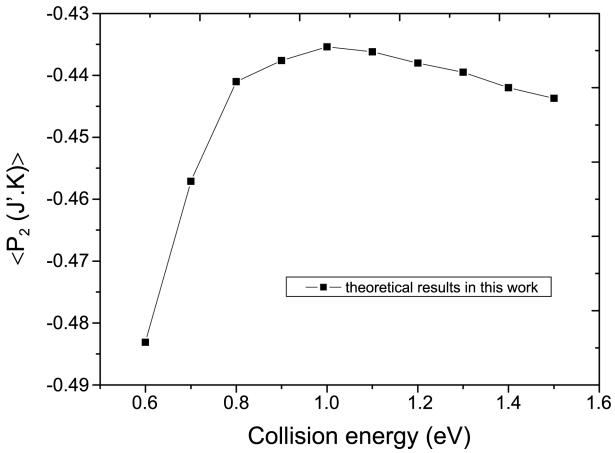

Figure 8. The product rotational alignment result of the reaction Ba + *m*-$C_6H_4CH_3Br$ *versus* collision energy.

which are shown in Figure 5 and Figure 6. However, it does not influence the results of $\langle P_2(\vec{J'}\cdot\vec{K})\rangle$ for the title reactions. The different mass combination is the main reason for the different values of the product rotational alignment.

It can be seen from Figure 7 and Figure 8 that the variation tendencies of the product rotational alignments for the reactions Ba + C_6H_5Br and Ba + *m*-$C_6H_4CH_3Br$ are similar with those of Figure 6 in Ref. (15), and the mass combinations of the two reactions basically belong to the type of Heavy + Light-Light (HLL) mass combination. The values of product rotational alignment for the reaction Ba + C_6H_5Br are overall bigger than those of Figure 6 in Ref. (15), and the alignment effects are not very strong. But the values of product rotational alignment for the reaction Ba + *m*-$C_6H_4CH_3Br$ are overall smaller and closer to the dynamics limit value –0.5, and the alignment effects are strong. For the reaction Ba + C_6H_5Br, the atomic mass of Ba is 137.327, the atomic mass of Br is 79.904, the atomic mass summation of the group C_6H_5 is 77.104, and the mass proportion of the reagents conforms to the HLL mass configuration. But for the reaction Ba + *m*-$C_6H_4CH_3Br$, the atomic mass summation of the group *m*-$C_6H_4CH_3$ is 91.130. The mass proportion of this reaction deviates from the HLL mass configuration and situates between the HLL mass configuration and the Heavy+Heavy-Light (HHL) mass configuration. Therefore, it can be seen that the different mass configurations have directly caused the different results in Figure 7 and Figure 8.

Conclusions

In summary, the studies by means of the QCT method for the reactions Ba + C_6H_5Br and Ba + *m*-$C_6H_4CH_3Br$ are carried out based on the constructed extended LEPS PESs. And the QCT results have been used to compare with and interpret the experimental results. It is shown that the theoretical results agree well with the experimental data of the two reactions even though the vibrational and rotational excitation states of the reagents are not considered here.

The results show that the peak values of the vibrational distributions of the products BaBr appear at around $v = 0$ when collision energies equal 1.09 and 1.10 eV, respectively. And these results all decrease with the increasing of vibrational quantum number. With the changes of collision energy from 0.6 to 1.5 eV, the reaction cross sections and the product rotational alignments for Ba + C_6H_5Br and Ba + *m*-$C_6H_4CH_3Br$ have been calculated in this paper. The cross section result of the reaction Ba + C_6H_5Br firstly increases to its maximum and then decreases with the increasing of collision energy. But the reaction cross section monotonously increases for the reaction Ba + *m*-$C_6H_4CH_3Br$. The cross section values of the reaction Ba + C_6H_5Br are bigger than those of the reaction Ba + *m*-$C_6H_4CH_3Br$, and this phenomenon is considered as that the existence of methyl can reduce the activity of atom Br. The product rotational alignment results all firstly rise and then fall with the increasing of collision energy. The values of $\langle P_2(\vec{J'}\cdot\vec{K})\rangle$ depend on the mass combination and the alignment effects of the reaction Ba + *m*-$C_6H_4CH_3Br$ are stronger than those of the reaction Ba + C_6H_5Br.

From the distributions of the two reactions studied in this paper, we arrive at the conclusions that the existence of methyl can bring some differences in the QCT results, and the reaction mechanism of the title reactions is different from that of the reactions between alkaline earth metal atom and halogenated alkane. In conclusion, the QCT calculated results of the title reactions are reasonably corresponding to the experiment.

Acknowledgments. This work was supported by the National Natural Science Foundation of China (11047110, 11105022 and 11147122), the Natural Science Foundation of Liaoning Province (Grant Nos. L2010055, L2010057, 201102016), and the Fundamental Research Funds for the Central Universities (2011QN060, 2011QN062, 2011JC021). The code used in this paper was provided by Professor Keli Han.

References

1. Han, K. L.; Mo, Y. X.; He, G. Z.; Lou, N. Q. *Chin. J. Chem. Phys.* **1990**, *3*, 157.
2. Han, K. L.; He, G. Z.; Lou, N. Q. *Science In China (Series B)* **1991**, *8*, 791.
3. He, G. X.; Wang, X. Y.; Li, F. E.; He, G. Z.; Lou, N. Q. *Chin. J. Chem. Phys.* **1991**, *4*, 319.
4. Han, K. L.; He, G. Z.; Lou, N .Q. *Chin. J. Chem. Phys.* **1991**, *4*, 241.
5. Li, R. J.; Han, K. L.; Li, F. L.; Lu, R. C.; He, G. Z.; Lou, N.Q. *Chem. Phys. Lett.* **1994**, *220*, 281.
6. Liu, Y. F.; Meng, H. Y.; Cong, S. L. *J. Atom. Mole. Phys.* **2005**, *22*, 119.
7. Han, K. L.; Zhang, L.; Xu, D. L.; He, G. Z.; Lou, N. Q. *J. Phys. Chem. A* **2001**, *105*, 2956.
8. Ma, J. J.; Cong, S. L.; Zhang, Z. H.; Wang, Y. Q. *Chin. J. Chem. Phys.* **2006**, *19*, 117.
9. Xia, W. W.; Lu, N.; Zhong, H. Y.; Yao, L. *Can. J. Chem*. **2009**, *87*, 1103.
10. Zhong, H. Y.; Xia, W. W.; Gu, L. Z.; Yao, L. *J. Theo. Comp. Chem.* **2009**, *8*, 861.
11. Xia, W. W.; Yao, L.; Chen, B. J. *J. Mol. Stru. (Theochem)* **2010**,

962, 56.
12. Yao, L.; Liu, Y. L.; Zhong, H. Y.; Cao, W. H. *J. Theo. Comp. Chem.* **2009**, *8*, 827.
13. Yao, L.; Zhong, H. Y.; Liu, Y. L.; Xia, W. W. *Chem. Phys.* **2009**, *359*, 151.
14. Han, K. L.; He, G. Z.; Lou, N. Q. *Chem. Phys. Lett.* **1991**, *178*, 528.
15. Han, K. L.; He, G. Z.; Lou, N. Q. *J. Chem. Phys.* **1996**, *105*, 8699.
16. Wang, M. L.; Han, K. L.; He, G. Z.; Lou, N. Q. *Bunsenges, Ber. Phys. Chem.* **1997**, *101*, 1527.
17. Zhang, X.; Xie, T. X.; Zhao, M. Y.; Han, K. L. *Chin. J. Chem. Phys.* **2002**, *15*, 169.
18. Frisch, M. J.; Trucks, G. W.; Schlegel, H. B. *Gaussian 03*, Revision A.1. Pittsburgh PA, 2003.
19. Porter, R. N.; Raff, M. L. In *Dynamics of Molecule Collision, Part B*; Miller, W. H., Ed.; Plenum Press: New York, 1976; p 1.
20. Costen, M. L.; Hancock, G.; Orr-Ewing, A. J.; Summerfield, D. *J. Chem. Phys.* **1994**, *100*, 2754.
21. Truhlar, D. G.; Muckerman, J. T. In *Atom-Molecule Collision Theory*; Bernstein, R. B., Ed.; Plenum Press: New York, 1976; p 505.
22. Han, K. L.; He, G. Z.; Lou, N. Q. *Chin. J. Chem. Phys.* **1989**, *2*, 323.
23. Prosant, M. G.; Rettner, C. T.; Zare, R. N. *J. Chem. Phys.* **1981**, *75*, 2222.
24. Cruse, H. W.; Dagdigian, P. J.; Zare, R. N. *Faraday Discuss. Chem. Soc.* **1973**, *55*, 277.
25. Han, K. L.; He, G. Z.; Lou, N. Q. *Chem. Phys. Lett.* **1993**, *203*, 509.